formed by gradual sapping as liquefied SO_2 seeps out at the base (*36*), perhaps exploiting and enlarging preexisting joints and fractures. The height of the mesa forming the eastern margin of Tvashtar Catena (Fig. 7) is ~1 km, the depth at which SO_2 is expected to become liquid (*30*). Diffuse white patches often appear to emanate from the bases of scarps on Io, consistent with plumes of SO_2 expected to form when the liquid reaches the triple point near Io's surface.

Discussion. The dominant eruption styles on Io may vary with latitude. At low latitudes, we see many long-lived eruptions with insulated flow fields and often associated with Prometheus-type plumes, as well as short-lived eruptive episodes (Pillan) and lava lakes (Pele). At high latitudes, the eruptions are mostly short-lived but high-volume outpourings of lava, probably with lava fountains such as that at Tvashtar (*27*). We have never seen an active plume at high latitudes, but we do see new color patterns indicative of short-lived plumes. One interpretation is that the lithosphere is thicker at high latitudes, such that only large batches of magma are able to ascend to the surface.

A subject of great interest for understanding global change is whether terrestrial flood lavas have been emplaced rapidly in open channels or sheet flows or relatively slowly through insulated (crusted-over) tubes or sheet flows (*37*). Most terrestrial flood lavas are highly eroded, so the emplacement style is contentious. On Io, we see examples of both rapidly emplaced flows (Pillan and Tvashtar) and flows emplaced over many years or decades (Zamama, Prometheus, Amirani, and Culann). These active flow fields provide important clues to the emplacement of ancient flood lavas on Earth and other planets. The formation and destruction of landforms such as mountains and calderas are also much more rapid on Io than on other planets, so Io is a unique laboratory to study processes normally inferred from the incomplete geologic record.

References and Notes

1. W. J. O'Neil *et al.*, in *The Flight of Project Galileo as Reported Annually to the IAF/AIAA, IAF-96-Q.2.01, 1* (International Astronautical Federation, Paris, 1997).
2. The majority of the I24 images were acquired in a special mode (2 × 2 pixel summation and a fast 2.6-s readout time) designed to minimize radiation noise. We expected the radiation noise to be severe in images acquired close to Io, but the image quality proved much better than expected. Unfortunately, the summation mode, which worked correctly through orbit C21, produced garbled images in I24. Many of the images were reconstructed with an innovative algorithm devised at the Jet Propulsion Laboratory (JPL) with the LabVIEW software from National Instruments (Austin, TX). However, the photometry remains severely compromised, eliminating useful color data, and parts of some images are completely unrecoverable. Full-resolution imaging modes (no pixel summing) worked correctly, but only a few partial (top one-third) frames were acquired in I24 while close to Io. I25 and subsequent encounters were replanned to acquire only full-resolution images.
3. See www.sciencemag.org/feature/data/1049308.shl for a table of I24 and I25 image characteristics and the Web figures.
4. A. S. McEwen *et al.*, *Icarus* **135**, 181 (1998).
5. R. Lopes-Gautier *et al.*, *Icarus* **140**, 243 (1999).
6. P. E. Geissler *et al.*, *Icarus* **140**, 265 (1999).
7. P. E. Geissler *et al.*, *Science* **285**, 870 (1999).
8. M. H. Carr *et al.*, *Icarus* **135**, 146 (1998).
9. A. S. McEwen *et al.*, *Science* **281**, 87 (1998).
10. T. V. Johnson and L. A. Soderblom, in *Satellites of Jupiter*, D. Morrison, Ed. (Univ. of Arizona Press, Tucson, AZ, 1982), pp. 634–646.
11. L. Keszthelyi and A. S. McEwen, *Icarus* **130**, 437 (1997); A. S. McEwen, R. Lopes-Gautier, L. Keszthelyi, S. W. Kieffer, in *Environmental Effects on Volcanic Eruptions: From Deep Oceans to Deep Space*, J. R. Zimbelman and T. K. P. Gregg, Eds. (Plenum, New York, in press).
12. Plumes have given names only (such as "Pele"), whereas surface features are called a patera (irregular or complex depression), fluctus (flow), mons (mountain), mensa (mesa), planum (plateau), or catena (chain). Most volcanic centers include several features, so in practice we often drop the feature name and refer to the entire complex by its given name.
13. J. R. Spencer *et al.*, *Geophys. Res. Lett.* **24**, 2471 (1997).
14. J. R. Spencer, K. L. Jessup, M. A. McGrath, G. E. Ballester, R. Yelle, *Science* **288**, 1208 (2000).
15. A. G. Davies *et al.*, *Lunar Planet. Sci.* **XXX** (1999) [CD-ROM].
16. L. Keszthelyi and A. S. McEwen, *Geophys. Res. Lett.* **24**, 2463 (1997).
17. C. B. Phillips, dissertation, University of Arizona, Tucson, AZ (2000).
18. L. Keszthelyi, A. S. McEwen, Th. Thordarson, *J. Geophys. Res.*, in press.
19. J. R. Spencer *et al.*, *Science* **288**, 1198 (2000).
20. S. Thorarinsson, *Bull. Volcanol.* **2**, 1 (1953).
21. D. A. Williams, A. H. Wilson, and R. Greeley, *J. Geophys. Res.* **105**, 1671 (2000); D. A. Williams *et al.*, *Eos* (spring meet. suppl.), in press.
22. K. Hon *et al.*, *Geol. Soc. Am. Bull.* **106**, 251 (1994); B. C. Bruno, G. J. Taylor, S. K. Rowland, P. G. Lucey, S. Self, *Geophys. Res. Lett.* **19**, 305 (1992).
23. T. N. Mattox, C. Heliker, J. Kauahikaua, K. Hon, *Bull. Volcanol.* **55**, 407 (1993).
24. R. Lopes-Gautier *et al.*, *Science* **288**, 1201 (2000).
25. S. W. Kieffer *et al.*, *Science* **288**, 1204 (2000).
26. D. S. Acton, M. E. Brown, B. F. Lane, in preparation.
27. J. A. Stansberry, J. R. Spencer, R. R. Howell, C. Dumas, D. Vakil, *Geophys. Res. Lett.* **24**, 2455 (1997).
28. S. A. Fagents, D. A. Williams, R. Greeley, *Eos* (fall meet. suppl.) **80** (no. 46), F625 (1999).
29. L. Wilson and J. W. Head, *Nature* **302**, 663 (1983); J. W. Head and L. Wilson, *Lunar Planet. Sci.* **XXXI** (2000) [CD-ROM].
30. S. W. Kieffer, in *Satellites of Jupiter*, D. Morrison, Ed. (Univ. of Arizona Press, Tucson, AZ, 1982), pp. 647–723.
31. S. E. Heslop, L. Wilson, H. Pinkerton, J. W. Head, *Bull. Volcanol.* **51**, 415 (1989).
32. J. S. Kargel, P. Delmelle, D. B. Nash, *Icarus* **142**, 249 (1999).
33. P. M. Schenk and M. H. Bulmer, *Science* **279**, 1514 (1998).
34. The compressive stress induced by globally uniform subsidence exceeds 1 kbar at a depth of 2.5 km. For comparison, the stresses induced by tides are expected to be between 2 and 6 bar.
35. J. M. Moore, R. J. Sullivan, R. T. Pappalardo, E. P. Turtle, *Lunar Planet Sci.* **XXXI** (2000) [CD-ROM].
36. J. F. McCauley, B. A. Smith, L. A. Soderblom, *Nature* **280**, 736 (1979).
37. S. Self, Th. Thordarson, L. Keszthelyi, in *Large Igneous Provinces: Continental, Oceanic, and Planetary Flood Volcanism*, J. J. Mahoney and M. F. Coffin, Eds. (American Geophysical Union, Washington, DC, 1997), pp. 381–410.

38. We thank J. Erickson and the Galileo team at JPL for their spacecraft recovery efforts during I24 and I25 and G. Levanus and G. Wells of JPL for the I24 image reconstruction.

8 February 2000; accepted 18 April 2000

Io's Thermal Emission from the Galileo Photopolarimeter-Radiometer

John R. Spencer,[1*] Julie A. Rathbun,[1] Larry D. Travis,[2] Leslie K. Tamppari,[3] Laura Barnard,[3] Terry Z. Martin,[3] Alfred S. McEwen[4]

Galileo's photopolarimeter-radiometer instrument mapped Io's thermal emission during the I24, I25, and I27 flybys with a spatial resolution of 2.2 to 300 kilometers. Mapping of Loki in I24 shows uniform temperatures for most of Loki Patera and high temperatures in the southwest corner, probably resulting from an eruption that began 1 month before the observation. Most of Loki Patera was resurfaced before I27. Pele's caldera floor has a low temperature of 160 kelvin, whereas flows at Pillan and Zamama have temperatures of up to 200 kelvin. Global maps of nighttime temperatures provide a means for estimating global heat flow.

The photopolarimeter-radiometer (PPR) is a simple aperture photometer on the Galileo scan platform, with a selection of broadband infrared filters including a wide-open filter that is sensitive to light over the full visible to 100-μm sensitivity range of the detector (*1*). During the close flybys (*2*), PPR obtained both dedicated raster scans of Io and "ride-along" sequences of data obtained simultaneously with the near-infrared mapping spectrometer (NIMS) or solid-state imaging (SSI) instruments. Calibration is with reference to dark sky and an onboard calibration source, and we estimate brightness temperatures (T_B's) to be accurate to within 10 K at 250 K and 5 K at 125 K (*3*).

[1]Lowell Observatory, 1400 West Mars Hill Road, Flagstaff, AZ 86001, USA. [2]Institute for Space Studies, NASA–Goddard Space Flight Center, 2880 Broadway, New York, NY 10025, USA. [3]Jet Propulsion Laboratory, 4800 Oak Grove Drive, Pasadena, CA 91109, USA. [4]Lunar and Planetary Laboratory, University of Arizona, Tucson, AZ 85721, USA.

*To whom correspondence should be addressed. E-mail: spencer@lowell.edu

Loki. Loki, Io's most powerful volcano, has been observed in continuous though variable activity since its discovery by Voyager. At wavelengths shortward of 5 μm, Loki shows >10-fold brightness variations, with well-defined "brightenings" occurring about once per year and lasting for several months (*4–6*). Previous observations have shown that the spatial extent of the hot materials coincides closely with the unique dark, lake-like area of Loki Patera seen in spacecraft images (*5*, *7*, *8*). Ground-based observations (*9*, *10*) show that a typical Loki brightening began between 25 August and 9 September 1999, and that Loki's 3.5-μm brightness had reached a plateau by the time of the I24 flyby on 11 October 1999.

On the I24 flyby, PPR obtained a nighttime map of the Loki region in its 17- and 21-μm filters (Fig. 1). The map shows that all the dark material of Loki Patera was hot, and the surrounding brighter material (and the bright "island" within the Patera) was much cooler. Most of Loki Patera had a uniform 17-μm T_B of 245 ± 10 K, consistent with uniform temperatures seen in Galileo NIMS observations of a small portion of Loki Patera taken after the PPR scan (*11*). NIMS obtained a 4.4-μm T_B of 273 K and a 4.1- to 4.7-μm color temperature of 305 K (*11*), while simultaneous PPR observations gave a 17-μm T_B of 247 K. These observations are approximately consistent with a model two-component blackbody with 88% of the surface at 236 K and 12% at 322 K. The effective temperature (T_E), the temperature of a blackbody emitting the same total power, was then 252 K.

The southwest part of Loki Patera [often the site of the brightest near-infrared emission (*12*, *13*)] was much hotter in I24, with T_B exceeding 370 K in an unresolved region, <20 km wide but elongated in a north-south direction, near 11.5°N, 309°W. West of the hottest region, temperatures were in the 330- to 370-K range, whereas to the east they dropped to the 250 K of the rest of the Patera in less than 20 km (*14*). The hot southwestern part of Loki Patera may be the site of the brightening that began in early September, and lava may have been spreading to the west (but not to the east) from a source at the hottest point. The temperature and area covered by >300-K material was consistent with expectations from simple models of cooling and spreading flows, with an areal production rate constrained by ground-based observations of Loki's 3.4-μm brightness (*15*, *16*). The lack of spreading to the west may indicate at least a temporary topographic barrier in that direction during I24. The uniform temperature of the rest of Loki Patera in I24 indicates either coverage by flows of roughly uniform age, or a uniform crust on a lava lake. The I24 T_E of 252 K ± 10 K (including the PPR calibration uncertainty) gives an age since resurfacing of 1 to 2 years, according to simple analytic silicate flow-cooling models that include insolation and assume a flow thick enough to be molten at depth (*16*). This age is approximately consistent with the hypothesis that these areas were last resurfaced in the previous Loki brightening of May to December 1998 (*9*, *10*). By I27 (Fig. 1, inset), toward the end of the ground-based Loki brightening, most of the previously isothermal portion of Loki Patera had increased in temperature by up to 40 K, so the lavas previously confined to the southwest of Loki Patera had apparently spread over most of the Patera by I27. However, there was no temperature peak during I27 at the site of the hottest I24 temperatures, which is puzzling if this was the source of the resurfacing magmas. Alternatively, the hottest I24 temperatures may represent a flow front (or possibly a line along which lava lake overturning was occurring) that moved to the east and north between I24 and I27.

Pele. PPR observed 17-μm nighttime thermal emission from Pele, the source of Io's largest persistent plume, at 3.5-km spatial resolution simultaneously with SSI (*17*) near I24 closest approach (Fig. 2). PPR saw a peak in temperature coinciding with the bright line of thermal emission seen by SSI. The peak T_B of about 200 K is almost certainly due to a much higher temperature filling a small fraction of the PPR field of view. To the east (concave side) of the bright line T_B averages 160 K, much higher than to the west of the line, supporting the SSI interpretation (*17*) that the bright line represents the southwestern edge of a warm crusted-over lava lake filling the Pele caldera. A second PPR peak was seen to the east of the SSI coverage, perhaps due to thermal emission from the east margin of the caldera; such a location would also be consistent with the SSI team's tentative registration of the high-resolution SSI images with low-resolution sunlit images (*17*). The 160-K temperature of the probable caldera floor is surprisingly low if the Pele caldera is an active lava lake, and indicates an age since resurfacing of many years (*16*) if the lava surface is solid rock. However, the incandescent margin to the caldera floor indicates a young, thin crust; the low temperature of the caldera floor may be due to coverage by insulating pyroclastic debris from the Pele plume, which was active during the I24 observations (*18*). At least some of Io's surface has a thermal conductivity as low as 320 erg cm^{-1} K^{-1} (*19*), and a 1-cm-thick layer of such material would be sufficient to reduce the crust surface temperature from 300 to 160 K, for example.

Pillan and Zamama. I24 PPR observations of Pillan, the site of a large, high-temperature eruption 2.3 years earlier (*20*), were obtained with 2.2-km resolution simultaneously with SSI images (*17*). A 17-μm T_B for the darkest flows, which probably date from the 1997 eruption, was 200 ± 20 K, whereas higher-albedo flows to the east of a prominent flow front were much colder, av-

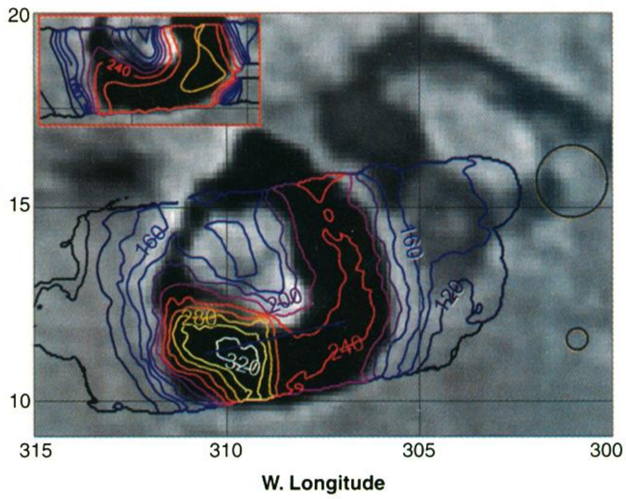

Fig. 1. PPR I24 17-μm nighttime brightness temperature map of Loki, superimposed on a Galileo visible-wavelength image. Field-of-view diameter varies from 60 to 20 km between the top and the bottom of the mosaic, as shown by the black circles on the right. The blue diagonal line shows the approximate location of the high-resolution temperature scan (*14*). The inset shows the same area during I27 in the wide-open filter at reduced scale but with the same contour color scheme.

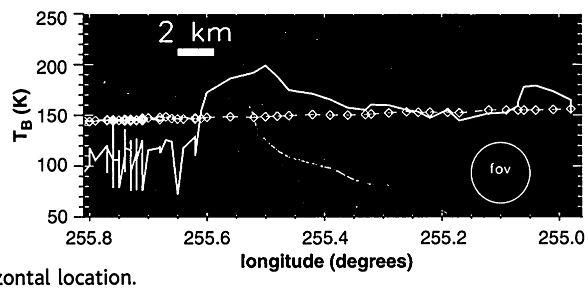

Fig. 2. Nighttime PPR scan of the Pele caldera, obtained simultaneously with the SSI images (*17*) in the background, which show only a single curving line of thermal emission. The diamonds show the location of the centers of the PPR fields of view (fov; size shown) relative to the image, while the solid line gives the brightness temperature of the PPR observation at the same horizontal location.

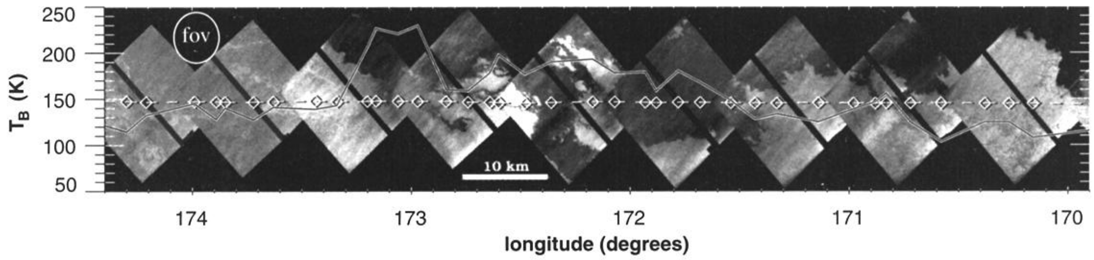

Fig. 3. PPR 17-μm scan across the flows of Zamama, superimposed on a simultaneous SSI mosaic (*17*). Details as in Fig. 2.

eraging 100 K. Cooling flow models (*16*) suggest that 2.3-year-old silicate flows will freeze to a depth of 13 m and, if thicker than 13 m, will have a surface temperature of 245 K. The lower observed temperatures may indicate that the flows have frozen completely, consistent with the thickness of only 10 m estimated from SSI images (*17*). The cold, high-albedo, eastern flows may date from a previous eruption or could be from an earlier stage of the 1997 eruption but covered with thick insulating pyroclastics from the plume that accompanied the eruption. The warmer flow may then have been erupted after pyroclastic activity ceased.

A similar I24 scan of the Zamama flow field (Fig. 3) showed that the dark flows there, which date from sometime between 1979 and 1996 (*12*), are also warm, with a temperature near 180 K. Howell's numerical flow models (*16*) extend only to 2.7 years of age, when the temperature is 240 K, so the observed temperatures of the Zamama flows indicate an age much greater than 2.7 years (consistent with the imaging evidence) or that the flows are thin enough to have frozen completely. Not all Zamama lavas are frozen, however, because there is continuing high-temperature activity in some parts of this volcanic complex (*12*, *21*, *22*). The highest T_B seen by PPR at Zamama is 225 K. From the sudden appearance and disappearance of this high temperature in the PPR field of view during the scan, we infer that it is due to a small unresolved region much hotter than 225 K. It corresponds not to a well-defined flow but rather to an area near the flow margin where surface detail appears to be obscured; this may be the source of an active plume, as has been seen before at Zamama (*12*).

Global nighttime temperatures and heat flow. PPR mapped thermal emission from 45% of Io's night side in its wide-open filter on I25 and I27, with a spatial resolution of 300 to 350 km. Emission from numerous hot spots is seen (Fig. 4), the brightest being Loki and Pillan, with a total power output of $1.2 \pm 0.3 \times 10^{13}$ and $3.0 \pm 0.5 \times 10^{12}$ W, respectively. Loki's power output is similar to that measured by Voyager in 1979 (1.5×10^{13} W) (*23*), whereas Pillan's large power output is probably radiated by the extensive flows erupted in 1997 and seen at high resolution in I24, and is thus of more recent origin. The very large, cool, hot spot associated with Lei-Kung Fluctus was not previously known, although NIMS and SSI have seen thermal emission from the southern end of this large flow (*12*, *21*). Lei-Kung has changed little in appearance since Voyager (*12*), and so is over 20 years old.

If we assume that all nighttime emission at temperatures above a model background temperature is volcanic, we can obtain a new estimate of Io's mean global volcanic heat flow from these data. PPR scans of smooth plains near Loki on I27 with 15-km resolution at 12°N latitude show uniform temperatures of 95 ± 2 km; the uniformity of these temperatures suggests that they are not contaminated by discrete hot spots and thus provide an estimate of passive background temperatures in this region. Assuming that passive nighttime temperatures have a $\cos^{1/4}$(latitude) dependence, as expected from the simplest models of equilibrium with sunlight, we then obtain a global mean heat flow of 2.0 ± 0.3 W m^{-2} if we assume that the area covered by PPR is representative of the entire area of Io, or 1.7 ± 0.3 W m^{-2} if we assume that Loki is unique and count its heat flow contribution only once. These numbers are slightly lower than other recent heat-flow estimates of 2.5 W m^{-2} (*4*) and 2.6 W m^{-2} (*23*). However, some low-latitude areas in Fig. 4, notably the pyroclastic ejecta deposits surrounding Pele, are colder than 95 K, showing that passive temperature distribution is more complex than indicated by our simple model. Also, Fig. 4 shows negligible dependence of temperature on latitude, so our assumption of a $\cos^{1/4}$(latitude) dependence of passive temperature results in much greater endogenic heat flow at high latitudes. Enhanced polar heat flow is predicted by some tidal heating models (*24*) but may not be not consistent with the observed uniform hot-spot distribution (*21*), so again our passive temperature model may be oversimplified. All

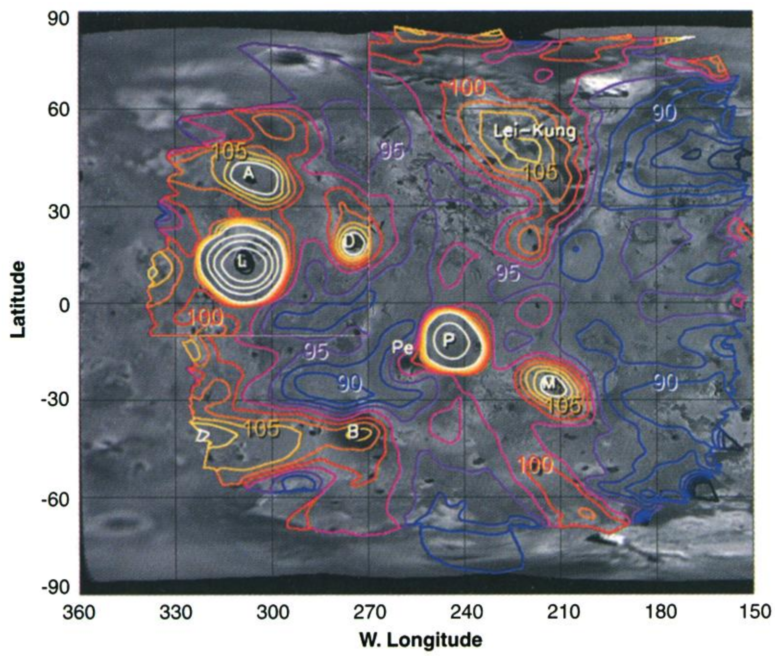

Fig. 4. Map of nighttime I27 and I25 (north and west of white line) T_B in PPR's wide-open filter superimposed on an SSI map of Io. Contour interval is 2.5 K below 110 K, 20 K above. Notable hot spots include Loki (L), Amaterasu (A), Daedalus (D), Pillan (P), Pele (Pe), Babbar (B), Marduk (M), Lei-Kung Fluctus, and many other fainter sources. Apparent high temperatures near the north pole, and possibly the low temperatures near 170°W, 40°N and 170°W, 30°S, may be spurious edge effects.

current heat-flow estimates are really lower limits, because they do not include heat conducted through the crust, which cannot be detected by current remote-sensing techniques.

References and Notes

1. E. E. Russell *et al.*, *Space Sci. Rev.* **60**, 531 (1992).
2. The close Io flybys were I24 on 11 October 1999, I25 on 26 November 1999, and I27 on 22 February 2000.
3. Brightness temperature is the temperature of a blackbody emitting the same radiance at the wavelength of interest, and is an approximation to the kinetic temperature for most solid surfaces, which exhibit near-blackbody behavior. Color temperature is the temperature of a blackbody emitting the same brightness ratio at a pair of wavelengths. Calibration accuracy can be judged by comparing the brightness temperature, T_B, of Loki Patera at the two independently calibrated wavelengths, 17 and 21 μm, for which we have resolved data. The closeness of the wavelengths, and the smoothness of Loki's spectrum from Voyager IRIS at these wavelengths (*16*), lead us to expect that T_B at the two wavelengths will differ by no more than 2 or 3 K. We obtain T_B of 244 K at 17 μm and 239 K at 21 μm for a representative region of the caldera, and thus conservatively estimate a 10-K temperature uncertainty at these temperatures. An additional check on calibration comes from simultaneous NIMS and PPR observations of another region of Loki Patera, for which PPR gives a 17-μm T_B of 247 K and NIMS gives a 4.4-μm T_B of 273 K, consistent with a two-temperature blackbody fit to NIMS and PPR data (see text). Observations of the onboard calibration target give an estimated T_B uncertainty of 5 K at the 125-K temperature of the target. Nighttime T_B in the wide-open filter on the Jupiter-facing hemisphere also includes a contribution from sunlight reflected from Jupiter; scaling from observations of Europa in the same filter (*25*), we estimate this contribution to be <2 K.
4. G. J. Veeder, D. L. Matson, T. V. Johnson, D. L. Blaney, J. D. Goguen, *J. Geophys. Res.* **99**, 17095 (1994).
5. J. R. Spencer, B. E. Clark, L. M. Woodney, W. M. Sinton, D. Toomey, *Icarus* **107**, 195 (1994).
6. J. R. Spencer *et al.*, *Geophys. Res. Lett.* **24**, 2451 (1997).
7. J. D. Goguen *et al.*, *Icarus* **76**, 465 (1988).
8. J. D. Goguen *et al.*, *Bull. Am. Astron. Soc.* **29**, 978 (1998).
9. R. R. Howell and A. J. Grocholski, *Lunar Planet. Sci.* **XXXI**, 1974 (2000) [CD-ROM].
10. J. R. Spencer, J. A. Stansberry, J. A. Rathbun, unpublished data.
11. R. Lopes-Gautier *et al.*, *Science* **288**, 1201 (2000).
12. A. S. McEwen *et al.*, *Icarus* **135**, 181 (1998).
13. B. MacIntosh *et al.*, in preparation.
14. Supplemental Web material is available at *Science* Online at www.sciencemag.org/feature/data/1050309.shl.
15. R. R. Howell, personal communication.
16. ———, *Icarus* **127**, 394 (1997).
17. A. S. McEwen *et al.*, *Science* **288**, 1193 (2000).
18. J. R. Spencer, K. L. Jessup, M. A. McGrath, G. E. Ballester, R. V. Yelle, *Science* **288**, 1208 (2000).
19. O. L. Hansen, *Icarus* **18**, 237 (1973).
20. A. S. McEwen *et al.*, *Science* **281**, 87 (1998).
21. R. Lopes-Gautier *et al.*, *Icarus* **140**, 243 (1999).
22. A. G. Davies *et al.*, *Geophys. Res. Lett.* **24**, 2447 (1997).
23. A. S. McEwen, N. R. Isbell, J. C. Pearl, *Lunar Planet. Sci.* **XXIII**, 881 (1992) [CD-ROM].
24. M. Segatz, T. Spohn, M. N. Ross, G. Schubert, *Icarus* **75** 187 (1988).
25. J. R. Spencer, L. K. Tamppari, T. Z. Martin, L. D. Travis, *Science* **284**, 1514 (1999).

26. We acknowledge the great efforts of the Galileo spacecraft team in making the Io encounters a success. R. Howell and R. Lopes provided valuable information and advice. Funded by the Galileo project and NASA grant NAG5 6794.

10 March 2000; accepted 19 April 2000

A Close-Up Look at Io from Galileo's Near-Infrared Mapping Spectrometer

Rosaly Lopes-Gautier,[1]* S. Douté,[2] W. D. Smythe,[1] L. W. Kamp,[1] R. W. Carlson,[1] A. G. Davies,[1] F. E. Leader,[2] A. S. McEwen,[4] P. E. Geissler,[4] S. W. Kieffer,[3] L. Keszthelyi,[4] E. Barbinis,[1] R. Mehlman,[2] M. Segura,[1] J. Shirley,[1] L. A. Soderblom[5]

Infrared spectral images of Jupiter's volcanic moon Io, acquired during the October and November 1999 and February 2000 flybys of the Galileo spacecraft, were used to study the thermal structure and sulfur dioxide distribution of active volcanoes. Loki Patera, the solar system's most powerful known volcano, exhibits large expanses of dark, cooling lava on its caldera floor. Prometheus, the site of long-lived plume activity, has two major areas of thermal emission, which support ideas of plume migration. Sulfur dioxide deposits were mapped at local scales and show a more complex relationship to surface colors than previously thought, indicating the presence of other sulfur compounds.

A major objective of the Galileo mission was to investigate Io's volcanoes and their surface modification processes using high spatial resolution spectral images. Observations were obtained during three flybys of Io in October (orbit I24) and November (orbit I25) of 1999 and February (I27) of 2000 using the near-infrared mapping spectrometer (NIMS). It was known previously that Io's surface is dotted with active volcanoes (hot spots) (*1*) and covered by SO_2 frost and other compounds (*2–4*). Some hot spots exhibit plumes that may inject gaseous SO_2 into the atmosphere (*5*), subsequently condensing as frost on the surface.

NIMS obtained 17 observations during I24, four observations during I25, and 10 observations during I27, most with spatial resolutions from 0.5 to 25 km/NIMS pixel. These were obtained at 14 fixed infrared (IR) wavelengths (in the range from 1.0 to 4.7 μm) instead of the planned 360, because the instrument's spectral scanning capability malfunctioned. This anomalous operation provided greater sampling density (24 samples instead of 1) at each wavelength, increasing the signal-to-noise ratio. The reduced number of wavelengths is suitable for temperature determination and SO_2 mapping, but our search for yet unknown surface compounds was compromised.

[1]Jet Propulsion Laboratory, California Institute of Technology, Pasadena, CA 91109, USA. [2]IGPP, University of California, Los Angeles, CA 90095, USA. [3]S. W. Kieffer Science Consulting Inc., 6 Queen Street, Suite 206, Post Office Box 520, Bolton, ON L7E 5T4 Canada. [4]Lunar and Planetary Laboratory, University of Arizona, Tucson, AZ 85721, USA. [5]U.S. Geological Survey, Flagstaff, AZ 86001, USA.

*To whom correspondence should be addressed. E-mail: rlopes@lively.jpl.nasa.gov

The NIMS spectral range includes reflected sunlight and thermal emission components (Web fig. 1) (*6*). A pixel showing volcanic activity may contain lavas at different temperatures (*7*), but here we use a single-temperature Planck function to estimate the brightness temperature T_B and the color temperature T_C, with a correction for reflected sunlight in daytime observations (*8*). T_B is a measure of the average emitted thermal energy within a given wavelength interval and pixel area. T_C uses the shape and amplitude of the Planck function to determine a temperature and its corresponding emitting area within the pixel. T_C estimates tend to be dominated by cooler materials that typically cover larger areas and thus emit greater power (in the wavelength range used) than hotter materials having much smaller areas.

For SO_2 mapping, the reduced number of wavelengths precluded the full-spectrum modeling used previously (*3*). We used the 4.1-μm spectral channel, which lies within the strong SO_2 $\nu_1 + \nu_3$ absorption band (Web fig. 1) (*6*), as a qualitative SO_2 indicator. Specifically, we form the relative band depth from the absorption depth at 4.1 μm relative to measurements at a nonabsorbing wavelength (3.0 μm) (*9*). The relative band depth depends on the SO_2 abundance, the mean grain size, and the presence of other materials and their mixing mode (spatially segregated or intimately mixed at the scale of photon path lengths). Here, we assume spatially segregated mixing. Sulfur dioxide absorbs strongly at 4.1 μm [absorption coefficient ~11 cm^{-1} (*10*)], so nonzero reflectance at that wavelength indicates the presence of other, nonabsorbing material. The assumption of spatially segregated mixing (*11*) with spectrally neutral material gives upper bounds to